doi:10.3847/2041-8205/825/1/L4

AGILE OBSERVATIONS OF THE GRAVITATIONAL-WAVE EVENT GW150914

M. Tavani[1,2,3], C. Pittori[4,5], F. Verrecchia[4,5], A. Bulgarelli[6], A. Giuliani[7], I. Donnarumma[1], A. Argan[1], A. Trois[8], F. Lucarelli[4,5], M. Marisaldi[6], E. Del Monte[1], Y. Evangelista[1], V. Fioretti[6], A. Zoli[6], G. Piano[1], P. Munar-Adrover[1], L. A. Antonelli[4,5], G. Barbiellini[9], P. Caraveo[7], P. W. Cattaneo[10], E. Costa[1], M. Feroci[1], A. Ferrari[11], F. Longo[9], S. Mereghetti[7], G. Minervini[12], A. Morselli[13], L. Pacciani[1], A. Pellizzoni[8], P. Picozza[13], M. Pilia [8], A. Rappoldi[10], S. Sabatini[1], S. Vercellone[14], V. Vittorini[1], P. Giommi[4], S. Colafrancesco[15], M. Cardillo[16], M. Galli[17], and F. Fuschino[18]

[1] INAF-IAPS, via del Fosso del Cavaliere 100, I-00133 Roma, Italy; victor@roma2.infn.it.it
[2] Dip. di Fisica, Univ.di Roma "Tor Vergata," via della Ricerca Scientifica 1, I-00133 Roma, Italy
[3] Gran Sasso Science Institute, viale Francesco Crispi 7, I-67100 L'Aquila, Italy
[4] ASI Science Data Center (ASDC), Via del Politecnico, I-00133 Roma, Italy
[5] INAF-OAR, via Frascati 33, I-00078 Monte Porzio Catone (Roma), Italy
[6] INAF-IASF-Bologna, Via Gobetti 101, I-40129 Bologna, Italy
[7] INAF-IASF Milano, via E.Bassini 15, I-20133 Milano, Italy
[8] INAF, Osservatorio Astronomico di Cagliari, Poggio dei Pini, strada 54, I-09012 Capoterra, Italy
[9] Dip. di Fisica, Universita' di Trieste and INFN, Via Valerio 2, I-34127 Trieste, Italy
[10] INFN-Pavia, Via Bassi 6, I-27100 Pavia, Italy
[11] CIFS, c/o Physics Department, University of Turin, via P. Giuria 1, I-10125, Torino, Italy
[12] Dip. di Matematica, Univ. di Roma "Tor Vergata," via della Ricerca Scientifica 1, I-00133 Roma, Italy
[13] INFN Roma Tor Vergata, via della Ricerca Scientifica 1, I-00133 Roma, Italy
[14] INAF/IASF-Palermo, Via U. La Malfa 153, I-90146 Palermo, Italy
[15] University of Witwatersrand, Johannesburg, South Africa
[16] INAF Osservatorio Astronomico di Arcetri, Largo Enrico Fermi, 5, I-50125 Firenze, Italy
[17] ENEA, Via Martiri Monte Sole 4, I-40129 Bologna, Italy
[18] Dipartimento di Fisica e Astronomia, Universitá di Bologna, viale Berti Pichat 6/2, I-40127 Bologna, Italy

Accepted 2016 May 12

ABSTRACT

We report the results of an extensive search through the *AGILE* data for a gamma-ray counterpart to the LIGO gravitational-wave (GW) event GW150914. Currently in spinning mode, *AGILE* has the potential of cover 80% of the sky with its gamma-ray instrument, more than 100 times a day. It turns out that *AGILE* came within a minute of the event time of observing the accessible GW150914 localization region. Interestingly, the gamma-ray detector exposed ∼65% of this region during the 100 s time intervals centered at −100 and +300 s from the event time. We determine a 2σ flux upper limit in the band 50 MeV–10 GeV, UL $= 1.9 \times 10^{-8}$ erg cm^{-2} s^{-1}, obtained ∼300 s after the event. The timing of this measurement is the fastest ever obtained for GW150914, and significantly constrains the electromagnetic emission of a possible high-energy counterpart. We also carried out a search for a gamma-ray precursor and delayed emission over five timescales ranging from minutes to days: in particular, we obtained an optimal exposure during the interval −150/−30 s. In all these observations, we do not detect a significant signal associated with GW150914. We do not reveal the weak transient source reported by *Fermi*-GBM 0.4 s after the event time. However, even though a gamma-ray counterpart of the GW150914 event was not detected, the prospects for future *AGILE* observations of GW sources are decidedly promising.

Key words: gamma rays: general – gravitational waves

1. INTRODUCTION

The recent discovery of gravitational waves (GWs) by the LIGO experiment impulsively emitted from the source GW150914 initiated a new era in astronomy (Abbott et al. 2016a, 2016b, 2016c, 2016d; hereafter A16a, A16b, A16c, A16d). The detection occurred at the beginning of an acquisition run of the LIGO experiment in an enhanced configuration (A16a). The LIGO-VIRGO detectors are expected to operate soon at even further improved sensitivity, and the potential for a large number of detections of gravitational phenomena will shape future ground-based and space research. The characteristics of gravitational phenomena emitting detectable GWs are those of the most extreme and energetic events of our universe. The energy radiated under the form of GWs, as inferred from GW150914, is about 3 $M_{\odot}$, a huge value (A16a). This energy was emitted during a few hundred milliseconds. It is clear that this type of gravitational phenomena opens the way to study the interplay between gravitation, the astrophysical context, and the quantum properties of fields and matter with unprecedented synergy. In general, GW-emitting final stages of coalescences involving compact stars (neutron stars (NSs) and black holes (BHs)) are the most likely candidates for LIGO-VIRGO events. X-ray and gamma-ray counterparts are expected from different types of coalescing compact star systems. The quest for electromagnetic (e.m.) counterparts to extreme gravitational events is now open.

The characteristics of the binary system associated with GW150914 are somewhat surprising given the current observations and understanding of the evolutionary processes leading to the formation of BHs. The event results from the coalescence of two BHs of relatively large masses (near 30 $M_{\odot}$) in an unknown stellar environment (A16d). Where and how such events can be produced is an open and interesting question (A16d): the physical conditions of the coalescing compact objects are far from being understood. Even though purely

gravity-systems such as BH–BH binaries are not anticipated to emit detectable e.m. radiation, nevertheless such radiation can be emitted before, during, and after coalescence, depending on the physical conditions of the system. It is then of great interest to explore this possibility and search for e.m. counterparts of GW events.

The *AGILE* satellite, today at its ninth year of operations in orbit, is observing the gamma-ray sky with excellent monitoring capabilities in the gamma-ray range 30 MeV–30 GeV. The satellite is currently in spinning mode, covering a large fraction of the sky with a gamma-ray sensitivity to transient emission that can reach flux levels near $F = (1–2) \times 10^{-8}$ erg cm^{-2} s^{-1} for ∼100 s integrations. This timescale is typical of passes of the imaging gamma-ray instrument (Field of View (FOV) of 2.5 sr) over exposed sky regions in spinning mode. Each accessible sky region is exposed more than 100 times a day[19] with 100 s integrations each. In addition, non-imaging detectors such as the *AGILE* Mini-Calorimeter (MCAL) and anticoincidence (AC) system (routinely employed for the detection of GRBs and Terrestrial Gamma-ray Flashes; TGFs) can be used. *AGILE* therefore has unique capabilities for searching for gamma-ray counterparts of GW sources.

In this letter we present the results of an extensive search through *AGILE* data for a high-energy counterpart to GW150914 that we performed retroactively once the event was made public.[20] The paper is organized as follows. In Section 2 we state the case for *AGILE* as an ideal space instrument for searching for gamma-ray counterparts to GW events. In Section 3 we present the results of *AGILE* observations and an extended analysis regarding the GW150914 event. In Sections 4 and 5 we briefly discuss our results and future perspectives. The sky exposure of *AGILE* and *Fermi*-GBM at the time of GW150914 is presented in the Appendix.

2. *AGILE*'S CAPABILITY FOR THE SEARCH OF GAMMA-RAY COUNTERPARTS OF GW SOURCES

The *AGILE* satellite, launched on 2007 April 23rd, orbits the Earth in a near equatorial orbit at a current altitude ∼500 km. The instrument consists of an imaging gamma-ray Silicon Tracker (sensitive in the energy range 30 MeV–30 GeV), Super-*AGILE* (currently working in rate-meter mode in the energy range 20–60 keV due to current temporary telemetry limitations), an MCAL (working in the range 0.4–100 MeV), and an AC system (for a summary of the *AGILE* mission features, see Tavani et al. 2009). The combination of Tracker, MCAL, and AC working as a gamma-ray imager constitutes the *AGILE*-GRID. The instrument is capable of detecting gamma-ray transients and GRB-like phenomena for timescales ranging from sub-milliseconds to ten-hundreds of seconds. In addition to the hundreds of GRBs detected by MCAL and Super-*AGILE*, several prominent GRBs were detected by the gamma-ray imager since the beginning of operations (GRB 080514B, Giuliani et al. 2008; GRB 090401B, Moretti et al. 2009; GRB 090510, Giuliani et al. 2010; GRB 100724B, Del Monte et al. 2011; GRB 130327B, Longo et al. 2013; GRB 130427A, Verrecchia et al. 2013; GRB 131108A, Giuliani et al. 2013 and Giuliani et al. 2015). Furthermore, *AGILE* has so far detected about 1000 TGFs with durations ranging from hundreds to thousands of microseconds (Tavani et al. 2011; Marisaldi et al. 2014). A special sub-millisecond search for transient events detected by MCAL is operational on board (Tavani et al. 2009).

The characteristics that make *AGILE* (in spinning mode) an important instrument for follow-up observations of large GW source localization regions are: (1) a very large FOV of the GRID (2.5 sr); (2) an accessible region of 80% of the whole sky that can be exposed every 7 minutes (see Figure 1); (3) 100–150 useful passes every day for any region in the accessible sky;[21] (4) a gamma-ray exposure of ∼2 minutes of any field in the accessible sky every 7 minutes, with a sensitivity reaching ∼10^{-8} erg cm^{-2} s^{-1} above 30 MeV for a typical single-pass of unocculted sky regions; (5) sub-millisecond trigger for very fast events detectable by MCAL in the range 0.4–100 MeV; (6) hard X-ray (20–60 keV) triggers of GRB-like events with a localization accuracy of 2–3 arcmin in the Super-*AGILE* FOV (∼1 sr) when operating in imaging mode.

Satellite data are transmitted to the ground currently on average every two consecutive passes over the Malindi ground station in Kenya. Scientific data are then processed by fast processing, typically producing alert for transient gamma-ray source and/or GRB-like events within 1.5–3 hr from satellite on-board acquisition (Pittori 2013; Bulgarelli et al. 2014).

3. *AGILE* OBSERVATIONS OF GW150914

The GW150914 event occurred at time $T_0 = 09{:}50{:}45$ UTC on 2015 September 14 (A16a). At that time *AGILE* was scanning the sky in spinning mode with the Earth only partially occulting the GRID FOV. Figure 2 shows the gamma-ray exposure above 50 MeV for the whole satellite 7 minute revolution that includes the GW150914 event time. As anticipated, the Earth only marginally covers the GW150914 localization region of the most accurate GW150914 localization map (LALInference, Veitch et al. 2015; Abbott et al. 2016e): most of the localization region is not occulted, and therefore available for *AGILE* exposure. We performed a search for: (1) the prompt event involving the GRID, MCAL, AC and Super-*AGILE* rate-meters (both inside and outside the GRID FOV); (2) delayed emission on multiple timescales involving the GRID; (3) precursor emission involving the GRID.

3.1. The Prompt Event

Figure 3 shows the gamma-ray exposure of a typical point inside the GW150914 localization region for the two satellite rotations of interest closer to the prompt event. *AGILE* had GRID exposure of a substantial fraction (65%) of the GW150914 localization region a few tens of seconds before T_0, but not at the event time (see also Figure 4). Had the instrument obtained an exposure of the field equal to that of a few tens of seconds earlier, *AGILE* could have obtained a gamma-ray sensitivity near 10^{-6} erg cm^{-2} s^{-1} for a brief integration in the range 50 MeV–10 GeV. A large fraction of the GW localization region was not occulted by the Earth and a strong X/gamma-ray signal, if any, could have been detected by the *AGILE* non-imaging detectors.

[19] Depending on Earth occultations and SAA passages.

[20] The *AGILE* Team was not part of the multifrequency follow-up collaboration with the LIGO-VIRGO team at the time of the GW150914 detection and subsequent investigations; we learned of the GW150914 event on 2016 February 11.

[21] The total number of 7 minute rotations is ∼200 day^{-1}; the useful number for gamma-ray exposure is affected by Earth occultations and SAA passages.

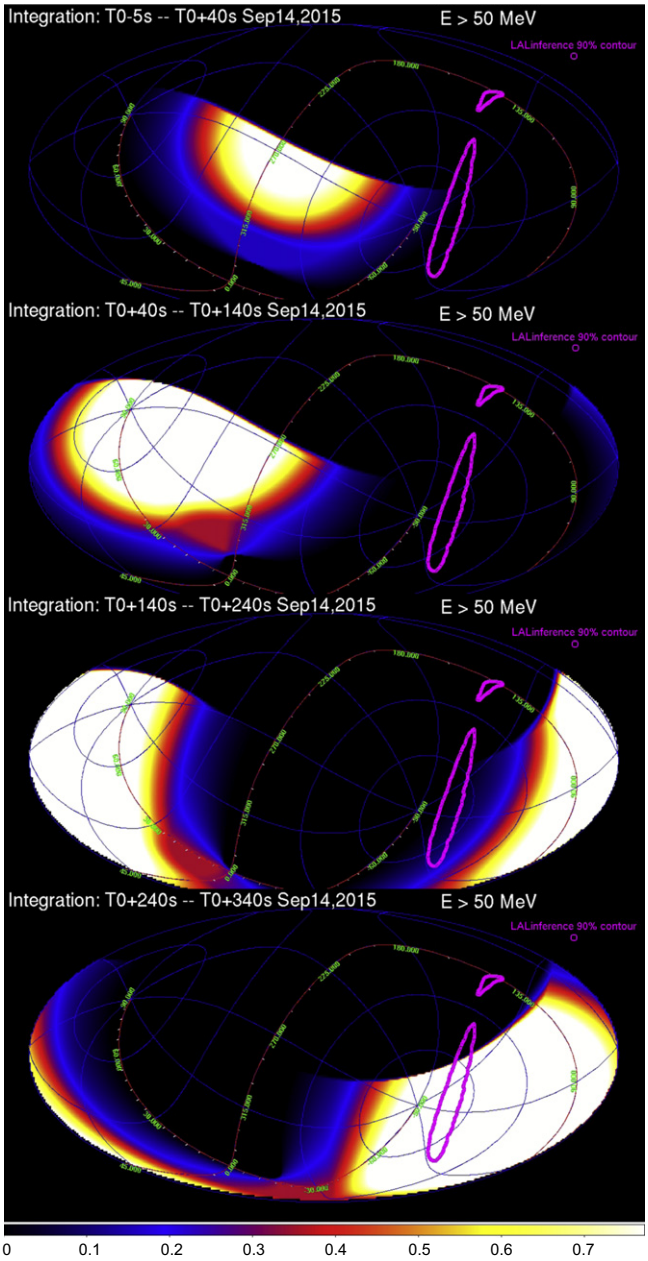

Figure 1. Hammer–Aitoff projection in Galactic coordinates of the *AGILE* satellite rotation and a typical sequence of $E > 50$ MeV gamma-ray exposure maps (in cm^2 s sr, using a 0.°5 pixel size) as the satellite rotates in spinning mode, scanning 80% of the sky in about 7 minutes. The *AGILE*-GRID FOV radius is assumed to be 70°. In this case, the Earth is occulting the FOV in the Northern Galactic hemisphere. The exclusion region for the albedo photons is 80° from the Earth center. This sequence applies to the satellite rotation that includes the prompt event time of GW150914 (localization region marked by the purple contour, LALinference 90% contour level, A16e).

AGILE-MCAL (Marisaldi et al. 2008; Labanti et al. 2009; Galli et al. 2013) is a scintillator detector that is sensitive in the 350 keV–100 MeV energy range, with an omnidirectional FOV without imaging capabilities. MCAL did not detect events above the onboard trigger threshold within the time interval covering $-100/+100$ s from T_0. Extending the MCAL search in the $-200/+200$ s from T_0 we found four events, all triggered at sub-millisecond or 1 ms timescales. Considering their characteristics, three events out of four can be disregarded as being due to instrumental noise, while one event is a candidate TGF. MCAL did not detect the transient reported by the *Fermi* GBM team (Connaughton et al. 2016) at $T_0 + 0.4s$ and possibly associated with GW150914. The LIGO-VIRGO and the GBM error boxes at time T_0 are viewed by MCAL at large off-axis angles between 90° and 120° (see the Appendix and Figure 7). This geometry is not favorable for MCAL detection; the MCAL effective area is a minimum at 90° off-axis angles, and for larger angles the uncertainties in the spacecraft mass model may play a role in the detector response matrix calculation, ultimately affecting the spectral reconstruction, especially at low energies. For the spectral shape reported in the GBM paper (best-fit single power law with an index of $-1.4^{+0.18}_{-0.24}$) we estimate an MCAL minimum fluence at a trigger threshold (five standard deviations above a background of ~600 counts s^{-1} near T_0) in the range $(2.0–6.7) \times 10^{-6}$ erg cm^{-2} in the 450–10,000 keV energy range, for a 1 s exposure in the 90°–120° off-axis angle range. This corresponds to an exposure between 67 and 220 cm^2 s in the same angular range. The estimated limit fluence is a factor 2.3 larger than the fluence reported for the *Fermi*-GBM event ($2.4^{+1.7}_{-1.0} \times 10^{-7}$ erg cm^{-2} in the 10–1000 keV energy range), when the difference in the energy range is accounted for. If we consider a typical Band spectral model (Band et al. 1993) for a short GRB (with parameters $\alpha = -0.5$, $\beta = -2.5$, and $E_{\mathrm{peak}} = 1000$ keV, as done in Savchenko et al. 2016) we can estimate the MCAL minimum fluence at the trigger threshold in the range $(1.9–5.1) \times 10^{-6}$ erg cm^{-2} in the 450–10,000 keV energy range, for a 1 s exposure in the 90°–120° off-axis angle range. This value agrees with the minimum MCAL fluence determined above.

A search in the Super-*AGILE* rate-meters data does not produce a significant detection with a 2σ fluence upper limit of 2.4×10^{-8} erg cm^{-2}. We note here that the interesting short GRB 090510 (Giuliani et al. 2010, see discussion below) is detected by the SA rate-meters with a significance level of $\sim 8.5\sigma$, although it occurred outside the 1 sr SA FOV. Also, a search for a signal in the AC data does not produce a significant detected flux.

AGILE was optimally positioned in the GW150914 localization region at interesting time intervals that preceded and followed the prompt event. The most interesting time intervals are during the time intervals $\Delta T_{-1} = -95 \pm 50$ s, and $\Delta T_{+1} = +333 \pm 50$ s, taking $T_0 =$ 09:50:45 UTC on 2015 September 14 as a time-zero reference. In the following, we focus on analyzing the gamma-ray data, searching for precursor and delayed gamma-ray emission. Table 1 shows the *AGILE*-GRID passing over the GW150914 localization region and shows the results of our analysis, in search of transient gamma-ray emission in that region.

3.2. A Search for Delayed Emission

The *AGILE*-GRID exposed a good fraction (75%) of the GW150914 localization region within 250 s from the prompt event. As shown in Figures 3 and 5, important information can be obtained during the first useful pass, ΔT_{+1}. Considering the local photon background and exposure, a search in the localization region for a transient gamma-ray source produces the 2σ UL for emission[22] in the range 50 MeV–10 GeV: UL $= 1.9 \times 10^{-8}$ erg cm^{-2} s^{-1}. This upper limit is significant

[22] For a hard spectrum similar to the short GRB delayed emission of GRB 090510 discussed below.

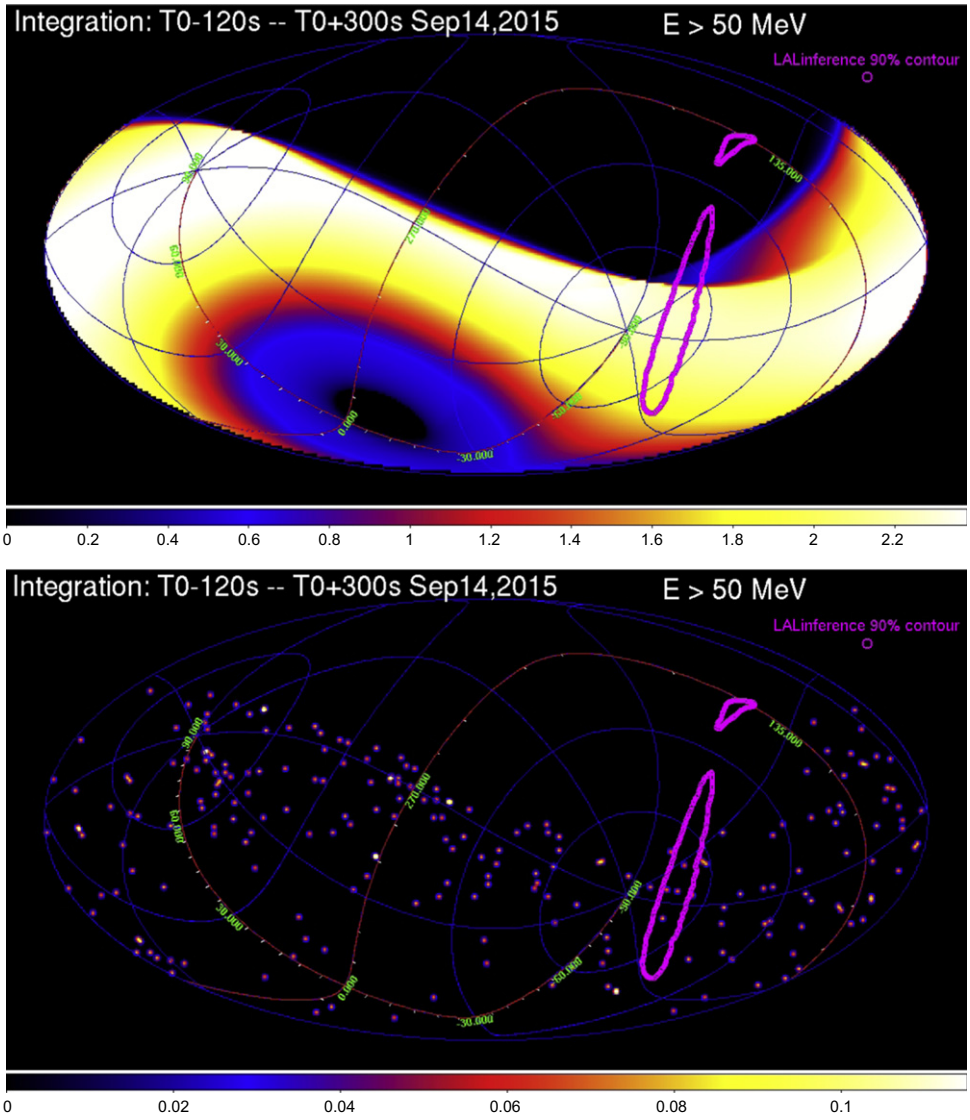

Figure 2. Hammer–Aitoff projection in Galactic coordinates. Top panel: *AGILE* cumulative gamma-ray exposure above 50 MeV (in cm^2 s sr, using a $0.^{\circ}5$ pixel size) during the satellite 7 minute rotation that includes the GW150914 event time. Bottom panel: gamma-ray photons above 50 MeV that were detected during the satellite 7 minute rotation. The GW150914 localization region is marked by the area inside the purple line (LALinference 90% contour level, A16e).

in the context of a possible gamma-ray signal from a cosmic event associated with compact object coalescence. Figure 6 shows the upper limit obtained by *AGILE* in the context of the gamma-ray light curve expected from the short GRB 090510 re-positioned at redshift $z = 0.09$ of GW150914. This short GRB, which shows several features expected from compact object coalescences possibly emitting GWs (e.g., Berger 2014), was detected by *AGILE* and *Fermi*-LAT with a significant delayed emission above 30 MeV, lasting up to 100 s with a hard spectral component (Abdo et al. 2009; Ackermann et al. 2010, and Giuliani et al. 2010). Thus, *AGILE* data uniquely determine a gamma-ray upper limit within 250–350 s from the GW150914 event.

Due to a temporary telemetry interruption caused by ground station operations in Malindi (Kenya), satellite data for two consecutive orbits following the interval ΔT_{+1} are not available. The next useful pass over the GW150914 localization region is about 3 hr after ΔT_{+1}, at $T = 10{,}800$ s after T_0.

We carried out a long-timescale search for transient gamma-ray emission during the hours immediately following the prompt event. No significant gamma-ray emission in the GW150914 localization region was detected during individual passes 3–4 hr after the GW150914 event.

We also performed a search on longer timescales up to several days after the event. Table 2 summarizes our results and upper limits for these long integrations.

3.3. A Search for a Gamma-Ray Precursor

An interesting possibility arises from the situation with two approaching massive BHs in a shrinking orbit. Even though current theoretical scenarios for BH–BH coalescences do not envision gamma-ray emission preceding or following the final event (e.g., Baumgarte & Shapiro 2011), a residual gaseous and/or plasma environment can in principle induce e.m. radiation during the approaching phase through non-thermal

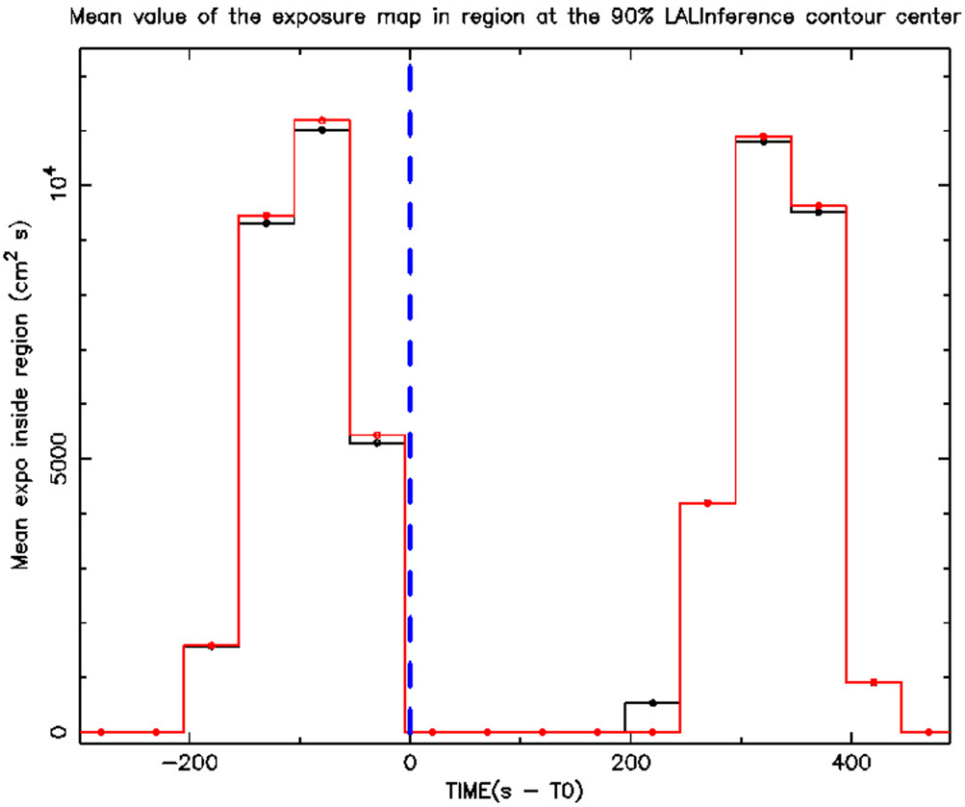

Figure 3. *AGILE* gamma-ray exposure above 50 MeV as a function of time for a region positioned at the center of the GW150914 localization region for the two passes, one preceding and one following the T_0 of GW150914. The GW150914 event time is marked by the dotted blue line. The black curve is obtained for a $7^\circ \times 25^\circ$ field centered at Galactic coordinates (l, b) = (282.8, −24.6). The red curve is obtained for a 10° radius circle centered at Galactic coordinates (l, b) = (283.5, −25.8).

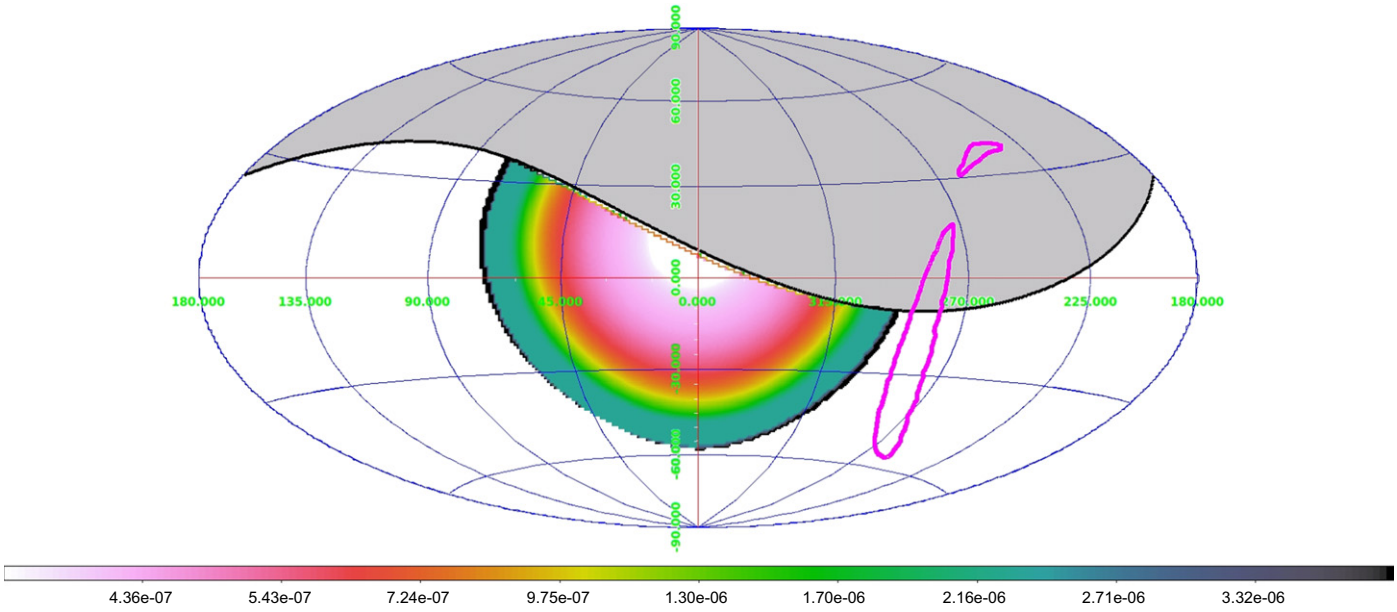

Figure 4. Hammer–Aitoff projection in Galactic coordinates of the *AGILE* gamma-ray sensitivity above 50 MeV (in erg cm^{-2} s^{-1}) during the 4 s interval that includes the GW150914 event time. The *AGILE*-GRID FOV is taken to be 70°. *AGILE* just missed covering the GW150914 localization region during the prompt event with useful sensitivity. The GW150914 localization region is marked by the purple contour (LALinference 90% contour level, A16e).

processes. In any case, this is relevant for determining if gamma-rays were emitted before the coalescence itself.

As reported in Tables 1 and 2, we carried out a search for a gamma-ray precursor over a large dynamic time range. The most significant observations are the available *AGILE*-GRID passes preceding the prompt event. Table 1 and Figure 5 show the sequence of passes. One of the most interesting passes is ΔT_{-1}, which covers the time interval -95 ± 50 s from T_0. The gamma-ray 2σ UL in this case is comparable with that obtained for the ΔT_{+1} interval, that is UL $= 1.5 \times 10^{-8}$ erg cm^{-2} s^{-1}.

Table 1
Analysis of Individual Passes over the GW150914 Localization Region

Interval Number	Central Time Bin[a]	Duration (s)	2σ UL[b] (10^{-8} erg cm^{-2} s^{-1})	Comments
−13	−5203	100	2.7	88% of error box not occulted
−12	−4779	100	⋯	affected by SAA
−11	−4355	100	⋯	affected by SAA
−10	−3931	100	⋯	affected by SAA
−9	−3507	100	⋯	affected by SAA
−8	−3083	100	2.3	93% of error box not occulted
−7	−2663	100	4.5	78% of error box not occulted
−6	−2235	100	1.5	68% of error box not occulted
−5	−1807	100	1.5	65% of error box not occulted
−4	−1379	100	1.5	20% of error box not occulted
−3	−951	100	1.0	48% of error box not occulted
−2	−523	100	1.0	56% of error box not occulted
−1	−95	100	1.5	65% of error box not occulted
+1	+333	100	1.9	75% of error box not occulted

Notes.
[a] Time calculated from T_0 = 09: 50: 45 UTC on 2015 September 14, the event time of GW150914.
[b] Flux upper limit obtained for emission in the range 50 MeV–10 GeV and for a spectrum similar to the delayed gamma-ray emission of the short GRB 090510.

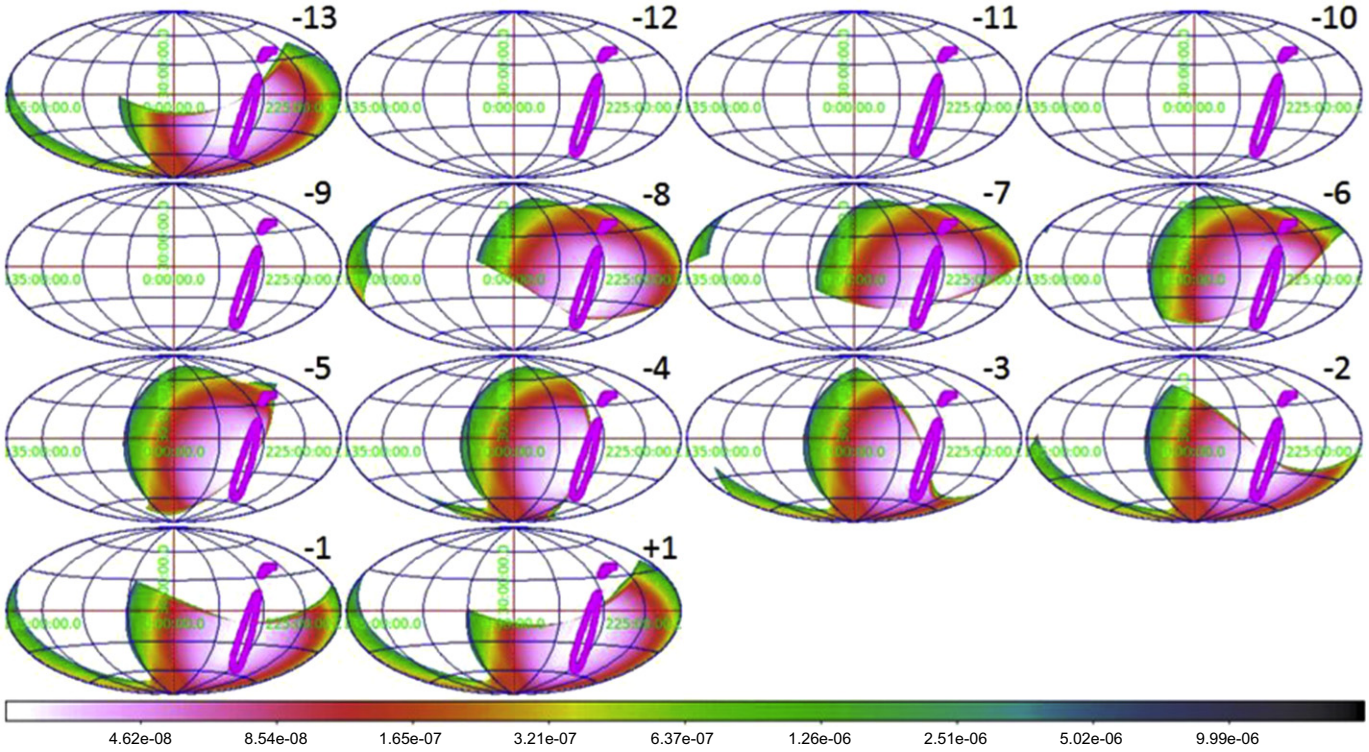

Figure 5. Sequence of ($E > 50$ MeV) maps in Galactic coordinates showing the *AGILE*-GRID passes with the best sensitivity over the GW150914 localization region obtained during the period (−5303, +433 s) with respect to T_0. The color maps show the gamma-ray flux 2σ upper limits in the range 50 MeV–10 GeV, with the most stringent values being UL = (1–2) × 10^{-8} erg cm^{-2} s^{-1}. The sequence shows 14 maps for all the 1-orbit passes of Table 1, corresponding to the 100 s interval numbers (from top left to bottom right): −13, −12, −11, −10, −9, −8, −7, −6, −5, −4, −3, −2, −1, +1. Note that the passes −12, −11, −10, −9 are blank (i.e., do not have appreciable exposure and therefore no reported ULs) because they are strongly affected by the SAA. The GW150914 localization region is marked by the purple contour (LALinference 90% contour level, A16e).

As Figure 5 shows, for the successive passes (retrograde in time) −2 and −3, the Earth progressively enters in the exposed GW150914 localization region. Passes −4 and −5 have a marginal exposure with a relatively high background because of the Earth albedo gamma-ray photons. The relevant region is then better exposed for intervals −6, −7, and −8. Interval −8 is one of the best cases, with more than 90% of the GW150914 localization region region well sampled. Unfortunately, the successive intervals −9, −10, −11, −12 are affected by a particularly deep passage in the SAA[23] and no useful data are

[23] Usually, passages into the SAA affect 1–2 rotations. In the period near T_0 of GW150914, the SAA passage was "deep" and affected four satellite rotations.

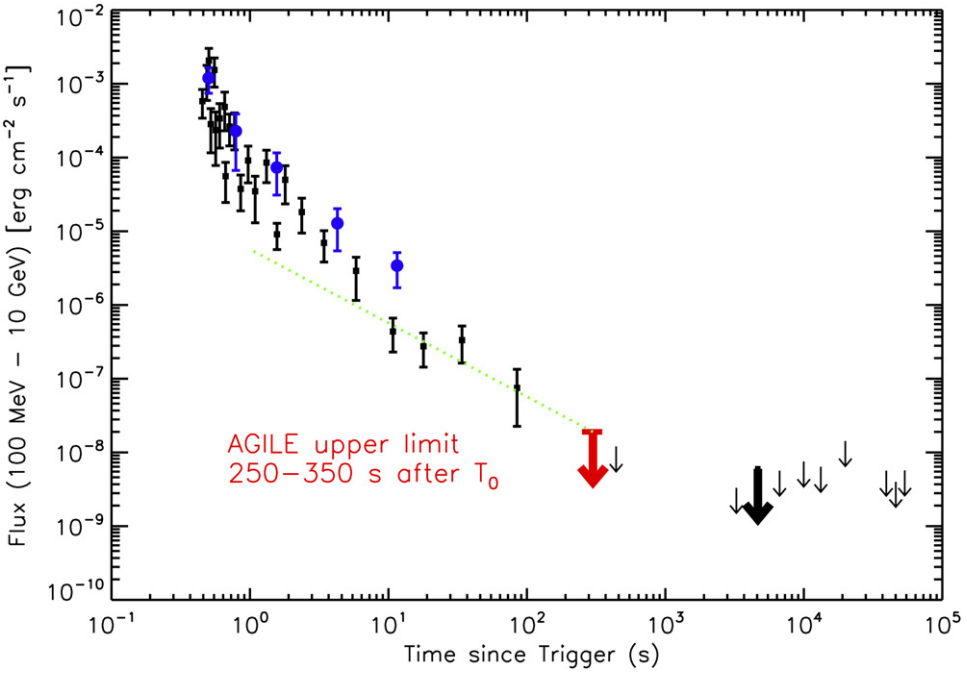

Figure 6. The *AGILE* (blue circles) and *Fermi*-LAT (black squares) gamma-ray light curves of the short GRB 090510 (originally at $z = 0.9$) scaled in flux and time-corrected as they it originated at the GW150914 luminosity distance of 400 Mpc ($z = 0.09$). The burst trigger time is assumed to be that of the GRB 090510 precursor occurring 0.53 s before the main hard X-ray event (see Ackermann et al. 2010; Giuliani et al. 2010). *Fermi*-LAT spectral data are from Fermi-LAT Collaboration (2016). The *AGILE* upper limit to gamma-ray emission above 100 MeV from the 65% of the GW150914 localization region during the time interval ΔT_{+1} is marked in red. The *Fermi*-LAT upper limit for GW150914, obtained in the interval 4442–4867 s after the event, is marked in black (Fermi-LAT Collaboration 2016). The green dotted curve shows the estimated *AGILE* gamma-ray UL derived by extrapolating the UL near 300 s back to 1 s.

Table 2
Long-integration Time Analysis of the GW150914 Localization Region

Interval Name	Duration	2σ UL[a] (10^{-9} erg cm^{-2} s^{-1})	Comments
−3d	3 days	0.3	···
−2d	2 days	0.5	···
−1d	1 day	0.7	···
−12h	12 hr	0.8	···
−6h	6 hr	2.5	···
−3h	3 hr	3.5	···
+3h	3 hr	···	telemetry interruption[b]
+6h	6 hr	3.5	with telemetry interruption[b]
+12h	12 hr	1.8	with telemetry interruption[b]
+1d	1 day	1.1	with telemetry interruption[b]
+2d	2 days	0.9	with telemetry interruption[b]
+3d	3 days	0.7	with telemetry interruption[b]
+5d	5 days	0.4	with telemetry interruption[b]

Notes.
[a] Gamma-ray upper limits (ULs) for photons in the range 100 MeV–10 GeV and for a E^{-2} spectrum obtained in the best exposed regions of the GW150914 localization region. We established a range of ULs within a factor of 2 inside the exposed localization region. The ULs were obtained by taking into account the effective exposure that has an overall efficiency near 70% due to Earth occultation and SAA passages.
[b] Telemetry interruption from UT 10:00 to UT 13:00 of 2015 September 14.

available for these intervals. Pass no. −13 is very similar to pass +1, and occurs after one orbit (∼95 minutes).

We also retroactively extended in time our search up to three days before T_0. No significant gamma-ray emission was detected during any time interval reported in Tables 1 and 2.

4. DISCUSSION

AGILE observed the field containing GW150914 with very good coverage and significant gamma-ray exposure within ten-hundreds of minutes before and after the event. The *AGILE*-GRID missed the coverage of the prompt event in its FOV, but could determine important limits immediately before and after the event. In light of the broad campaign of follow-up observations of the GW150914 localization region ranging from radio to gamma-rays reported in Abbott et al. (2016e), the *AGILE* observations are significant in providing the fastest response to the event with optimal gamma-ray sensitivity.

The most important result of the *AGILE* observations is the gamma-ray UL close to 10^{-8} erg cm^{-2} s^{-1} in the range 50 MeV–10 GeV obtained in the interval 250–350 s after T_0. It is interesting to compare this UL with other observations obtained by imaging X-ray/gamma-ray space instruments with FOVs larger that 1 sr. The BAT instrument on board the *Swift* satellite could not observe the GW150914 field because it occurred outside its FOV (Evans et al. 2016). The same applies to *Fermi*-LAT, which could not cover the GW150914 localization region at the moment of the prompt event (Fermi-LAT Collaboration 2016). Compared with the *Fermi*-LAT gamma-ray UL that was obtained more than 70 minutes after the event (Fermi-LAT Collaboration 2016), the *AGILE*-GRID observation at ΔT_{+1} provides a more stringent constraint to any delayed emission above 50 MeV shortly after the event.

We note that "delayed" gamma-ray emission is sometimes detected from both long and short GRBs (e.g., Ackermann et al. 2010; De Pasquale et al. 2010; Giuliani et al. 2010). In particular, the case of the gamma-ray bright short GRB 090510 is relevant to our purposes because of its characteristics and its possible association with a compact star coalescence involving

GW emission. The event, localized through its afterglow at $z = 0.9$, showed a first quasi-thermal interval lasting about 300 ms, with a spectrum peaking at a few MeV, and a second "gamma-ray afterglow" phase lasting hundreds of seconds that was detected above 100 MeV with a highly non-thermal spectrum (Ackermann et al. 2010; Giuliani et al. 2010). The possibility of detected delayed gamma-rays from GRBs is of great relevance for detectors such as the *AGILE*-GRID. As shown in Figure 6 the *AGILE* UL obtained 300 s after the GW event is just below the gamma-ray emission expected from a short GRB 090510-like event relocated at the distance of $z = 0.1$. Our data are close to excluding a delayed gamma-ray afterglow of the same type as GRB 090510. We note that if a short GRB of this kind were positioned at 400 Mpc, it would have been detectable by the *AGILE* non-imaging detectors (AC, MCAL, and Super-*AGILE* rate-meters) as well as by *Fermi*-GBM and *INTEGRAL*/SPI-ACS, if the event had the same hard X-ray spectrum as GRB 090510. We checked that the current sensitivity of the *AGILE* AC system is about a factor of 5–10 better than the flux detected in the case of the short GRB 090510, implying that a signal 10 times weaker than that associated with GRB 090510 would have been detected.

Also of interest is the limit obtained 50–100 s before the coalescence. For a total mass near $60\,M_{\odot}$, we are sampling the radiative environment when the orbital distance a is $\sim(0.1–1)\,R_{\odot}$. We are excluding precursor gamma-ray activity at the distance comparable with the solar size during the compact object approach. If dynamically formed in a dense stellar environment, the BH–BH binary associated with GW150914 might carry a gaseous remnant with it as a product of the three-body encounter that formed the binary. This gaseous component is subject to the gravitational influence of the approaching massive BHs and can settle into a short-lived disk that might produce e.m. radiation by thermal and non-thermal processes. The observed flux UL translates into an upper limit to the (isotropically) radiated gamma-ray luminosity, $L_{\gamma} < 3 \times 10^{47}\,\mathrm{erg\,s^{-1}}$, assuming the GW150914 luminosity distance of ∼400 Mpc. For a duration of 100 s, this corresponds to a limit to the radiated gamma-ray energy, $E_{\gamma} \sim 1.7 \times 10^{-5}\,M_{\odot}$.

AGILE does not detect the very weak event reported by *Fermi*-GBM about 0.4 s after T_0 (Connaughton et al. 2016). The MCAL did not register any event above the trigger threshold in the energy range 0.4–100 MeV, and the AC and Super-*AGILE* detectors did not register enhancements of their count rates during the GW150914 prompt event (in the ranges 80–200 keV and 20–60 keV, respectively). Considering the faintness and spectrum of the *Fermi*-GBM event[24] this lack of detection is not surprising.

5. FUTURE OBSERVATIONS

In the near future, we expect a relatively large number of aLIGO and aLIGO-VIRGO detections of GW sources. As the GW sensitivity and event positioning is improving, the capability of alerting the community within timescales that are progressively shorter is hoped for. With aLIGO-aVIRGO being capable of detecting NS–NS and NS–BH coalescing systems, the likelihood of detecting e.m. emission from these events will increase substantially.

We showed in this paper that *AGILE* can effectively observe relatively large sky regions associated with GW events with high efficiency. As demonstrated in the case of GW150914, *AGILE* might obtain significant results if the event occurs in the accessible sky region, which depends on the sky coverage per 7 minute rotation (∼0.8) and Earth occultation (∼0.6), with a probability of $\sim 0.8 \times 0.6 \simeq 0.5$. In this case, *AGILE* can obtain imaging gamma-ray data within a timescale ranging from seconds to 300–400 s. This is exactly the case that occurred for GW150914. The GRID FOV just missed the prompt event, and had exposure for most of the localization region only ∼300 s after T_0. As shown in Section 2, this is the worst case that could have happened given the conditions. Nevertheless, the upper limit obtained for this "late" exposure provides the fastest data in constraining the GW150914 e.m. emission.

The probability of catching the "prompt" event in the GRID FOV is about 0.2 within the duration of the *AGILE* satellite spinning rotation. The overall probability for *AGILE* to have good exposure of the FOV during the prompt phase of a GW event is then $\sim 0.5 \times 0.2 = 0.1$. This is a relatively large probability compared to other satellites or ground instruments.

Further improvement of the efficiency and speed of the *AGILE* data processing is a task for the near future. The *AGILE*-GRID data management system allows us to obtain results within ∼2 hr of the onboard data acquisition (Pittori 2013; Bulgarelli et al. 2014). The data processing can be further optimized for a fast search of gamma-ray transients within a selected sky region communicated by an external alert. Super-*AGILE*, MCAL, and AC data can be used in conjunction with GRID data to improve the search for transients. In addition, the reactivation of Super-*AGILE* data telemetry will make possible an event localization with 2 arcmin accuracy. The prospects for future follow-up gamma-ray observations of GW sources by *AGILE* are bright.

AGILE is an ASI space mission developed with programmatic support by INAF and INFN. We acknowledge partial support through the ASI grant no. I/028/12/0.

APPENDIX
MCAL VISIBILITY VERSUS *FERMI*-GBM FOR THE PROMPT EVENT

It is interesting to compare, taking into account the Earth occultation at the prompt time of GW150914, the sky accessible to the *AGILE* MCAL and AC detectors, as well as to the *Fermi*-GBM detector as reported by Connaughton et al. (2016). Figure 7 shows, in Galactic coordinates, the sky region accessible at the prompt time of GW150914 by *AGILE* detectors and by *Fermi* detectors. It turns out that at T_0 the non-imaging detectors of *AGILE* and *Fermi* were differently observing the sky. From Figure 7 we deduce that the *AGILE* MCAL and AC detectors exposed the "lower" part of the GW150914 localization region (in Galactic coordinates). *Fermi*-GBM instead exposed the "upper" part of the GW150914 localization region. A central part of the localization region was simultaneously exposed by MCAL and GBM. This jointly exposed region includes the best position of the transient reported by Connaughton et al. (2016), albeit with poor exposure. As discussed in the main text, neither *AGILE*'s

[24] This latter event was also not confirmed by the *INTEGRAL* SPI-ACS observation covering the GW150914 prompt event (Savchenko et al. 2016). The SPI-ACS upper limit is important since it is obtained by another satellite not occulted by the Earth at the time of T_0. The analysis of the SPI-ACS instrument is reported in the interval from −30 to +30 s from T_0.

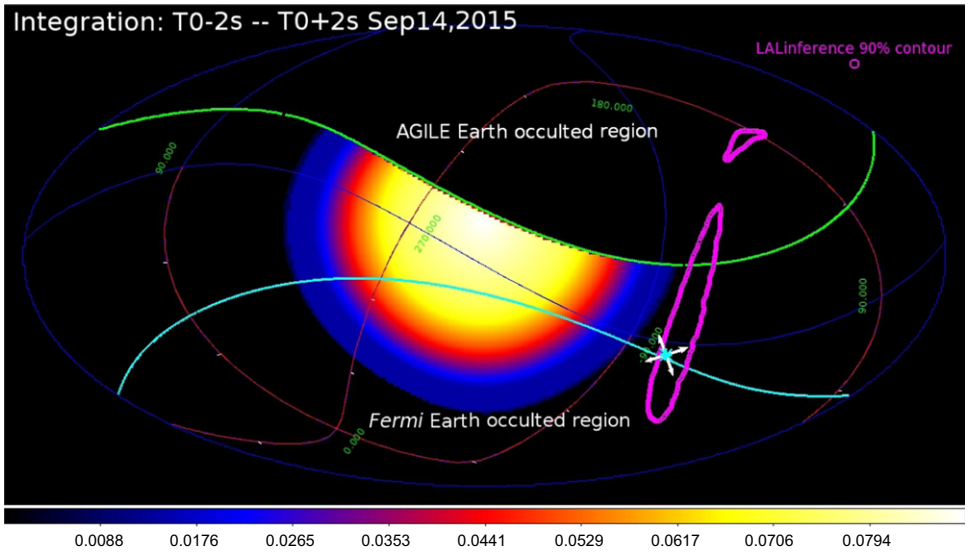

Figure 7. Comparison between the unocculted sky regions of *AGILE* and *Fermi* at the time of the GW150914 prompt event. Hammer–Aitoff projection in Galactic coordinates of the *AGILE* gamma-ray exposure above 50 MeV during the 4 s interval that includes the GW150914 event time. The *AGILE*-GRID FOV is taken to be 70°. The Earth occultation region for *AGILE* covers the upper hemisphere, with the boundary marked in green. The GW150914 localization region is marked by the purple contour (LALinference 90% contour level, A16e). The map also shows the Earth occulted region for *Fermi* as deduced from Connaughton et al. (2016), whose boundary is marked by the light blue line. This occulted region covers the lower region of the hemisphere. The white cross marks the position of the most probable position of the *Fermi*-GBM event detected 0.4 s after T_0 (Connaughton et al. 2016).

MCAL nor AC detected emission on or near the GW150914 prompt event.

REFERENCES

Abbott, B. P., Abbott, R., Abbott, T. D., et al. 2016a, PhRvL, 116, 061102
Abbott, B. P., Abbott, R., Abbott, T. D., et al. 2016b, Observing Gravitational-Wave Transient GW150914 With Minimal Assumptions [LIGO-P1500229]
Abbott, B. P., Abbott, R., Abbott, T. D., et al. 2016c, GW150914: First Results from the Search for Binary Black Hole Coalescence with Advanced LIGO [LIGO-P1500269-v12]
Abbott, B. P., Abbott, R., Abbott, T. D., et al. 2016d, Properties of the Binary Black Hole Merger GW150914 [LIGO-P1500218]
Abbott, B. P., Abbott, R., Abbott, T. D., et al. 2016e, ApJL, submitted
Abdo, A. A., Ackermann, M., Ajello, M., et al. 2009, Natur, 462, 331
Ackermann, M., Asano, K., Atwood, W. B., et al. 2010, ApJ, 716, 1178
Band, D., Matteson, J., Ford, L., et al. 1993, ApJ, 413, 281
Baumgarte, T. W., & Shapiro, S. 2011, PhT, 64, 32
Berger, E. 2014, ARA&A, 52, 43
Bulgarelli, A., Trifoglio, M., Gianotti, F., et al. 2014, ApJ, 781, 19
Connaughton, V., Burns, E., Goldstein, A., et al. 2016, ApJL, in press (arXiv:1602.03920)
Del Monte, E., Barbiellini, G., Donnarumma, I., et al. 2011, A&A, 535, A120
De Pasquale, M., Schady, P., Kuin, N. P. M., et al. 2010, ApJL, 709, L146
Evans, P. A., Kennea, J. A., Barthelmy, S. D., et al. 2016, MNRAS, in press (arXiv:1602.03868)
Fermi-LAT Collaboration 2016, ApJ, submitted (arXiv:1602.04488v2)
Galli, M., Marisaldi, M., Fuschino, F., et al. 2013, A&A, 553, A33
Giuliani, A., et al. 2015, A&A, submitted
Giuliani, A., Fuschino, F., Vianello, G., et al. 2010, ApJL, 708, L84
Giuliani, A., Longo, F., Verrecchia, F., et al. 2013, GCN, 15479, 1
Giuliani, A., Mereghetti, S., Fornari, F., et al. 2008, A&A, 491, L25
Labanti, C., Marisaldi, M., Fuschino, F., et al. 2009, NIMPA, A598, 470
Longo, F., Giuliani, A., Marisaldi, M., et al. 2013, GCN, 14344, 1
Marisaldi, M., Fuschino, F., Tavani, M., et al. 2014, JGR, 119, 1337
Marisaldi, M., Labanti, C., Fuschino, F., et al. 2008, A&A, 490, 1151
Moretti, E., Longo, F., Barbiellini, G., et al. 2009, GCN, 9069, 1
Pittori, C. 2013, NuPhS, 239, 104
Savchenko, V., Ferrigno, C., Mereghetti, S., et al. 2016, ApJL, submitted (arXiv:1602.04180v1)
Tavani, M., Barbiellini, G., Argan, A., et al. 2009, A&A, 502, 995
Tavani, M., Marisaldi, M., Labanti, C., et al. 2011, PhRvL, 106, 8501
Veitch, J., Raymond, V., Farr, B., et al. 2015, PhRvD, 91, 042003
Verrecchia, F., Pittori, C., Giuliani, A., et al. 2013, GCN, 14515, 1